SEMILEPTONIC DECAYS OF D MESONS

Written January 2008 by Lawrence Gibbons (Cornell Univ.) and Milind V. Purohit (Univ. of South Carolina).

I. Introduction and theory

Semileptonic decays of hadrons involve the interaction of a leptonic current with a hadronic current, as shown in Fig. 1. The simplicity of the leptonic current allows us to use measurements of semileptonic decays to obtain the form factors that describe the nonperturbative hadronic current [1]. Conversely, because the leptonic and hadronic final-state systems do not interact, semileptonic decays for which the form factors can be predicted provide a powerful means for obtaining CKM matrix elements [2].

From general considerations such as Lorentz invariance, the matrix element $\mathcal{M}$ for the semileptonic decay of a D meson, $D \to M\ell\nu$, must have the form

$$\mathcal{M} = -i\frac{G_F}{\sqrt{2}} V_{cq} L^\mu H_\mu, \tag{1}$$

where G_F is the Fermi constant and V_{cq} is a CKM matrix element. The leptonic current L_μ can be evaluated directly from the lepton spinors, while the hadronic current H_μ requires a fundamentally nonperturbative QCD calculation. Lorentz invariance, however, implies that we can parametrize H_μ in terms of the independent four-momenta and polarizations in the process. The nonperturbative form factors are functions of the hadronic momentum transfer squared: $q^2 = W^{*2} \equiv (p_\ell + p_\nu)^2$, where p_ℓ and p_ν are the four momenta of the charged lepton and the neutrino, and W^* is the virtual $W^\pm$.

For a decay $D \to P\ell\nu$, where D and P are pseudoscalars, H_μ is purely a vector current, and can be represented by two form factors, with $f_+(q^2)$ and $f_0(q^2)$ a typical choice. Then

$$H_\mu = \left\langle P(p)|\bar{q}\gamma^\mu c|D(p')\right\rangle =$$

$$f_+(q^2)\left[(p'+p)^\mu - \frac{(M_D^2 - m_P^2)}{q^2}q^\mu\right] + f_0(q^2)\frac{(M_D^2 - m_P^2)}{q^2}q^\mu . \tag{2}$$

Here M_D and p' are the mass and four momentum of the parent D meson, m_P and p are those of the final-state meson, and $q = p' - p$. Kinematics constrains $f_+(0)$ to equal $f_0(0)$.

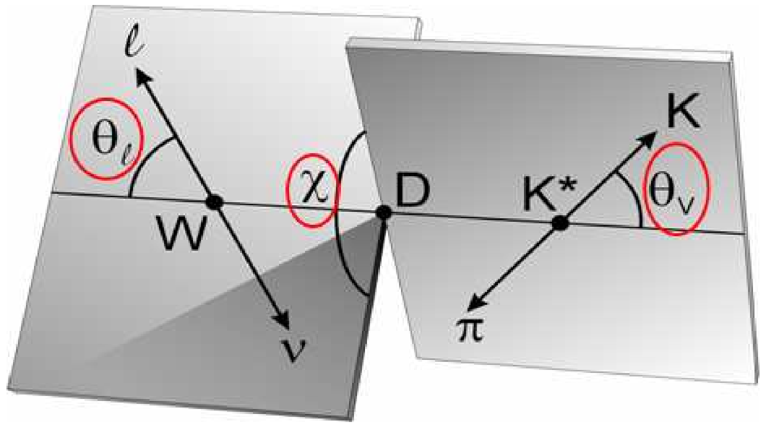

Figure 1: Decay angles θ_V, θ_ℓ, and χ, defined for $D^+ \to K^* \ell^+ \nu_\ell$. The angle χ between the decay planes shown is defined in the D^+ reference frame, while the other angles are defined in the hadronic and leptonic center-of-mass frames.

A decay $D \to V \ell \nu$, where V is a vector meson, can proceed through both axial and vector currents, and the polarization vector ε of the V enters the parametrization; there are altogether four form factors. A common choice [3] represents the vector current as

$$V_\mu = \left\langle V(p,\varepsilon)|\bar{q}\gamma^\mu c|D(p')\right\rangle = \frac{2V(q^2)}{M_D + m_h}\varepsilon_{\mu\nu\rho\sigma}\varepsilon^{*\nu} p'^\rho p^\sigma, \tag{3}$$

and the axial current as

$$\begin{aligned} &A_\mu = \left\langle V(p,\varepsilon)| - \bar{q}\gamma^\mu\gamma^5 c|D(p')\right\rangle = \\ &-i(M_D + m_h)A_1(q^2)\varepsilon^*_\mu + i\frac{A_2(q^2)}{M_D + m_h}(\varepsilon^* \cdot q)(p' + p)_\mu + \\ &i\frac{2m_h}{q^2}\left(A_3(q^2) - A_0(q^2)\right)[\varepsilon^* \cdot (p' + p)]q_\mu \ . \end{aligned} \tag{4}$$

Here m_V is the mass of the V meson, and

$$A_3(q^2) = \frac{(M_D + m_V)}{2m_V}A_1(q^2) - \frac{(M_D - m_V)}{2m_V}A_2(q^2). \tag{5}$$

Kinematics constrains $A_3(0)$ to equal $A_0(0)$.

When the charged lepton is light (an e or μ), contributions to the partial width involving $q^\mu L_\mu$ give rise to terms proportional to the lepton mass [3], so vanish in the limit $m_\ell \to 0$. Then the pseudoscalar decay can effectively be described in terms of the single form factor $f_+(q^2)$, and the vector decay in terms of the three form factors, $V(q^2)$, $A_1(q^2)$, and $A_2(q^2)$. In this limit, the differential partial widths, integrated over various angular distributions, become

$$\frac{d\Gamma(D \to P\ell\bar{\nu}_\ell)}{dq^2\, d\cos\theta_\ell} = \frac{G_F^2|V_{cq}|^2}{32\pi^3} p^{*3}|f_+(q^2)|^2 \sin\theta_\ell^2, \tag{6}$$

$$\frac{d\Gamma(D \to V\ell\bar{\nu}_\ell)}{dq^2\, d\cos\theta_\ell} = \frac{G_F^2|V_{cq}|^2}{128\pi^3 M_D^2} p^* q^2 \times$$

$$\left[\frac{(1-\cos\theta_\ell)^2}{2}|H_-|^2 + \frac{(1+\cos\theta_\ell)^2}{2}|H_+|^2 + \sin^2\theta_\ell |H_0|^2\right]. \tag{7}$$

Here p^* is the (q^2-dependent) magnitude of the 3-momentum of the decay meson in the D rest frame. The dependence on the angle θ_ℓ between the charged lepton in the virtual W rest frame (see Fig. 1) and the direction of the virtual W^* results directly from the $V-A$ structure of the $W \to \ell\bar{\nu}_\ell$ process. In $D \to P\ell\nu$ decay, the W^* can only be longitudinally polarized and the angular dependence is independent of the nonperturbative dynamics; this gives a powerful experimental cross-check or constraint. In $D \to V\ell\nu$ decay, all W^* polarizations are allowed and there are three helicity amplitudes:

$$H_\pm(q^2) = \frac{(M_B + m_V)^2 A_1(q^2) \mp 2M_D p^* V(q^2)}{M_D + m_V}$$

$$H_0(q^2) = \frac{1}{\sqrt{q^2}} \frac{M_B^2}{2m_V(M_D + m_V)} \times$$

$$\left[\left(1 - \frac{m_V^2 - q^2}{M_D^2}\right)(M_D^2 + m_V^2)A_1(q^2) - 4{p^*}^2 A_2(q^2)\right] \tag{8}$$

The left-handed nature of the quark current manifests itself as $|H_-| > |H_+|$. This implies a charged-lepton momentum spectrum in $D \to \overline{V}\ell\nu$ decay that is softer than the neutrino spectrum.

Experimentally, one must understand the q^2 dependence ("shape") of the form factors (and their relative normalizations in vector decay) to evaluate reconstruction efficiencies. Extraction of the CKM matrix element requires knowledge of the absolute normalization of the form factors. Conversely, precise studies of the form-factor shapes and normalizations (with CKM elements input from other measurements) provide a crucial check of the theoretical approaches to nonperturbative calculations, such as lattice QCD (LQCD) or Light Cone Sum Rules.

Form-factor parametrizations

Various parametrizations of form factors have been introduced to try to capture the fundamental strong dynamics of the decay, while allowing comparisons of a small number of parameters between different experiments and between theory and experiment. Typically, a parametrization takes advantage of dispersion relations (see, *e.g.*, Ref. [4]) , which allow expression of a form factor in terms of an explicit pole and a sum of effective poles:

$$f(q^2) = \frac{f(0)}{(1-\alpha)} \frac{1}{1 - \frac{q^2}{m^2_{\rm pole}}} + \sum_{k=1}^{N} \frac{\rho_k}{1 - \frac{1}{\gamma_k} \frac{q^2}{m^2_{\rm pole}}}, \tag{9}$$

Here $m_{\rm pole}$ is the mass of the lowest-lying $c\bar{q}$ resonance expected to make the largest contribution to the form factor (at least near $q^2_{\rm max}$), given the underlying $c \to q$ quark transition. For the $D \to \pi$ transition involving a vector current, for example, the D^* meson should dominate. The parameter α determines the fractional contribution from the dominant resonance at $q^2 = 0$, and the ρ_K and γ_K are expansion parameters for the effective poles.

Pole-motivated parametrizations

Using the dispersion relation, the form factor can be approximated to any desired accuracy by keeping enough terms in the expansion. However, in this approach, the decay dynamics are not explicitly predicted, and the convergence properties are not manifest.

Omitting the sum over effective poles in Eq. (9) is an approximation called "nearest-pole dominance" or "vector-meson dominance." The resulting form factor is

$$f_+(q^2) = \frac{f_+(0)}{(1 - q^2/m^2_{\rm pole})}. \tag{10}$$

However, values of $m_{\rm pole}$ that fit the data do not agree with the expected vector meson masses [5]; see the next Section.

The modified-pole, or Becirevic-Kaidalov (BK), parametrization [6], keeps the first term of the effective pole expansion, but makes additional assumptions to allow expression of the form factor with only two parameters: the intercept $f_+(0)$ and a shape parameter, α_{BK}. The BK parametrization takes the form

$$f_+(q^2) = \frac{f_+(0)}{(1 - \frac{q^2}{m^2_{\rm pole}})(1 - \alpha_{BK}\frac{q^2}{m^2_{\rm pole}})}. \tag{11}$$

For the ansatz to be self-consistent, α_{BK} should be near 1.75. However, values of α_{BK} that fit the data are nowhere near 1.75 (see the next Section).

z expansion

Several groups have advocated a different series expansion for the physical description of heavy-meson form factors [1,4,7,8]. The expansion is congruous with the dispersion relations, yet provides a systematic framework for improving the precision to which a form factor is described.

To obtain a convergent series, the expansion is formulated as an analytic continuation of the form factor into the complex $t = q^2$ plane. The branch cut on the real axis for $t > (M_D + m_h)^2$ is mapped onto the unit circle by the variable z, defined as

$$z(q^2, t_0) = \frac{\sqrt{t_+ - q^2} - \sqrt{t_+ - t_0}}{\sqrt{t_+ - q^2} + \sqrt{t_+ - t_0}}\ ; \tag{12}$$

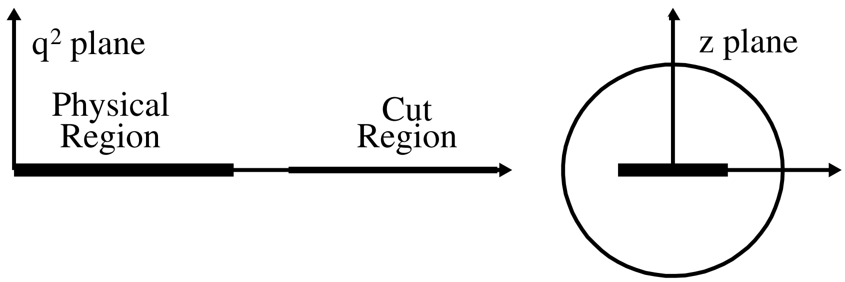

Figure 2: The transformation from q^2 to the z variable.

see Fig. 2. Here $t_\pm \equiv (M_D \pm m_h)^2$ and t_0 is the (arbitrary) q^2 value that maps to $z = 0$. The expression for a form factor becomes

$$f(q^2) = \frac{1}{P(q^2)\phi(q^2, t_0)} \sum_{k=0}^{\infty} a_k(t_0)[z(q^2, t_0)]^k. \tag{13}$$

The $P(q^2)$ factor accommodates sub-threshold resonances, thus solving the convergence issues that a naive expansion would face with a nearby pole. For example,

$$P(q^2) \equiv \begin{cases} 1 & \text{for } D \to \pi \\ z(q^2, M^2_{D_s^*}) & \text{for } D \to \overline{K}. \end{cases} \tag{14}$$

The "outer" function, $\phi(t, t_0)$, can be any analytic function. A standard choice (*e.g.* [4,7,9]) arises from considerations of unitarity and the perturbative OPE, and leads to the parameter constraint (at $1/m_c$) $\sum_{k=0}^{n_a} a_k^2 \leq 1$.

Good convergence properties are expected since the physical region is restricted to $|z| < 1$. The physical observables do not depend on the choice of $\phi(q^2, t_0)$ or on the value of t_0. In fact, choosing $t_0 = t_+\left(1 - \sqrt{1 - t_-/t_+}\right)$ minimizes the maximum value that z can assume. For $D \to \pi \ell \bar{\nu}$, for example, this choice implies that $|z| < 0.17$ [5].

II. Semileptonic decays to pseudoscalar mesons

As noted above, $D \to Pe\nu$ and $D \to P\mu\nu$ decays can be well described by a single form factor, $f_+(q^2)$. Corrections for the finite μ mass in the $D \to P\mu\nu$ decays only become noticeable at low q^2 [10], while corrections for $D \to Pe\nu$ decays are negligible everywhere. Recent experiments studying the f_+ form factor for D^0 and D^+ decays to $\overline{K}\ell\nu_\ell$ and $\pi\ell\nu_\ell$ have moved beyond the simple pole-dominance model and give information about the modified pole parametrization and, in some cases, the z-expansion parametrization.

Pole parametrizations

Measurements of the effective pole mass in the simple pole model and of the $\alpha_{\rm BK}$ parameter in the modified pole model are given for $D \to \overline{K}\ell\nu$ and $D \to \pi\ell\nu$ in Table 1 and are shown in Fig. 3.

As is clear from Fig. 3, the $\overline{K}\ell\nu$ data yield pole masses that are significantly lower than the mass of the D_s^* resonance that should dominate in the vector-dominance (simple-pole) model; and $\pi\ell\nu$ data suggest a pole mass that is lower than the D^* mass. The simple-pole parametrizations can usually provide good fits to the data, but low pole masses indicate that higher-mass resonances and the DK and $D\pi$ continuum make non-negligible contributions.

The BK parametrization adds an effective single-parameter correction to the leading physical pole in an attempt to account for these secondary contributions. The fits, however, yield values of $\alpha_{\rm BK}$ that are far smaller than the value $\alpha_{\rm BK} \approx 1.75$ that would be consistent with the assumptions that lead to the simplified form.

The recent unquenched form-factor calculations by the combined Fermilab lattice, MILC, and HPQCD groups for $D \to \overline{K}/\pi\ell\bar{\nu}$ [17] also yield an α_{BK} value. The chiral extrapolation to physical light-quark masses for these calculations uses the BK parametrization for intermediate interpolation as a function of K or π energy, effectively building the form into the final form-factor prediction. There are differences between the experimental results and the values derived from the LQCD

Table 1: Results for $m_{\rm pole}$ in the simple pole model, and for $\alpha_{\rm BK}$ in the BK-modified model for $D \to \overline{K}\ell^+\nu$ and $D \to \pi\ell^+\nu$ decays. Also given are lattice QCD predictions.

$D \to \overline{K}\ell\nu$ or $\pi\ell\nu$	Ref.	$m_{\rm pole}({\rm GeV}/c^2)$	$\alpha_{\rm BK}$
CLEO III ($D^0 \to K^-$)	[11]	$1.89 \pm 0.05^{+0.04}_{-0.03}$	$0.36 \pm 0.10^{+0.03}_{-0.07}$
FOCUS ($D^0 \to K^-$)	[10]	$1.93 \pm 0.05 \pm 0.03$	$0.28 \pm 0.08 \pm 0.07$
Belle ($D^0 \to K^-$)	[12]	$1.82 \pm 0.04 \pm 0.03$	$0.52 \pm 0.08 \pm 0.06$
BaBar ($D^0 \to K^-$)	[13]	$1.884 \pm 0.012 \pm 0.016$	$0.377 \pm 0.023 \pm 0.031$
CLEO-c ($D^0 \to K^-$)	[14]	$1.943^{+0.037}_{-0.033} \pm 0.011$	$0.258^{+0.063}_{-0.065} \pm 0.020$
CLEO-c ($D^0 \to K^-$)	[16]	$1.97 \pm 0.03 \pm 0.01$	$0.21 \pm 0.05 \pm 0.03$
CLEO-c ($D^+ \to K_S$)	[14]	$2.02^{+0.07}_{-0.06} \pm 0.02$	$0.127^{+0.099}_{-0.104} \pm 0.031$
CLEO-c ($D^+ \to K_S$)	[16]	$1.96 \pm 0.04 \pm 0.02$	$0.22 \pm 0.08 \pm 0.03$
Ferm. lattice/MILC/HPQCD	[17]	–	0.50 ± 0.04
CLEO III ($D^0 \to \pi^-$)	[11]	$1.86^{+0.10+0.07}_{-0.06-0.03}$	$0.37^{+0.20}_{-0.31} \pm 0.15$
FOCUS ($D^0 \to \pi^-$)	[10]	$1.91^{+0.30}_{-0.15} \pm 0.07$	–
Belle ($D^0 \to \pi^-$)	[12]	$1.97 \pm 0.08 \pm 0.04$	$0.10 \pm 0.21 \pm 0.10$
CLEO-c ($D^0 \to \pi^-$)	[14]	$1.941^{+0.042}_{-0.034} \pm 0.009$	$0.20^{+0.10}_{-0.11} \pm 0.03$
CLEO-c ($D^0 \to \pi^-$)	[16]	$1.87 \pm 0.03 \pm 0.01$	$0.37 \pm 0.08 \pm 0.03$
CLEO-c ($D^+ \to \pi^0$)	[14]	$1.99^{+0.11}_{-0.08} \pm 0.06$	$0.05^{+0.19}_{-0.22} \pm 0.13$
CLEO-c ($D^+ \to \pi^0$)	[16]	$1.97 \pm 0.07 \pm 0.02$	$0.14 \pm 0.16 \pm 0.04$
Ferm. lattice/MILC/HPQCD	[17]	–	0.44 ± 0.04

chiral extrapolation procedure. Since with $\alpha_{\rm BK}$ we are examining more directly corrections to the leading pole behavior of f_+, the discrepancies may have their origin in the nonphysical description of the form factor coupled with differing experimental (and lattice) sensitivities across the q^2 range.

***z* expansion results**

The z expansion allows the introduction of shape parameters in a controlled fashion. BaBar [13] and CLEO-c [16] have analyzed form factors using the first three terms of Eq. (14): a_0 controls the absolute normalization of $f_+(q^2)$, and a_1 and a_2 control its q^2 dependence. Table 2 gives the values of the normalized shape parameters $r_1 = a_1/a_0$ and $r_2 = a_2/a_0$. The BaBar correlation coefficient was obtained by refitting their

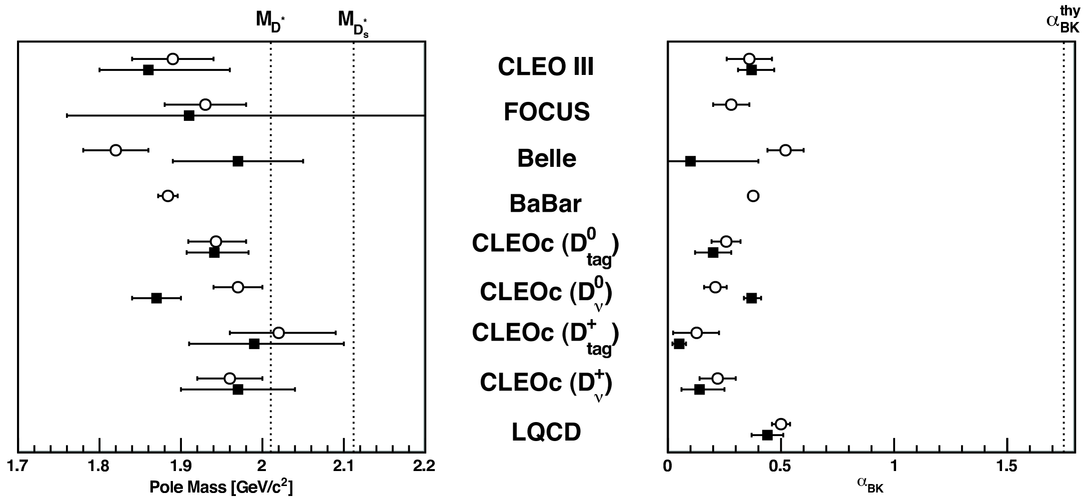

Figure 3: Effective pole masses for the simple pole parameterization fits (left), and the $\alpha_{\rm BK}$ parameter for the modified pole parameterization fits (right). $K\ell\nu$ results are shown as open circles; $\pi\ell\nu$ results are shown as closed squares. Unless indicated otherwise, the measurements are for D^0 decay.

published branching-fraction information with their published total covariance matrix.

Table 2: Values of $r_1 = a_1/a_0$ and $r_2 = a_2/a_0$ from z expansions. The correlation coefficient ρ is for the total uncertainties (statistical + systematic) on r_1 and r_2.

Expt.	Mode	Ref.	r_1	r_2	ρ
BaBar	$D^0 \to K^-$	[13]	$-2.5 \pm 0.2 \pm 0.2$	$1 \pm 6 \pm 5$	-0.64
CLEO-c	$D^0 \to K^-$	[16]	$-2.4 \pm 0.4 \pm 0.1$	$21 \pm 11 \pm 2$	-0.81
Average	$D^0 \to K^-$		-2.3 ± 0.23	5.9 ± 6.3	-0.74
CLEO-c	$D^+ \to K_S$	[16]	$-2.8 \pm 6 \pm 2$	$32 \pm 18 \pm 4$	-0.84
CLEO-c	$D^0 \to \pi^+$	[16]	$-2.1 \pm 7 \pm 3$	$-1.2 \pm 4.8 \pm 1.7$	-0.96
CLEO-c	$D^+ \to \pi^0$	[16]	$-0.2 \pm 1.5 \pm 4$	$-9.8 \pm 9.1 \pm 2.1$	-0.97

The values listed correspond to the choice

$$t_0 = t_+ \left(1 - \sqrt{1 - t_-/t_+}\right),$$

which minimizes the maximum value that $|z|$ can obtain. The standard outer function $\phi(q^2, t_0)$ given in Eq. (14) is used.

For the $D^0 \to K^- \ell^+ \nu$ measurements, the 68% and 96% probability contours (assuming Gaussian errors) are shown in Fig. 4. The agreement between BaBar and CLEO-c in data improves over the 2.5 standard deviation discrepancy seen in α_{BK}.

Table 2 also gives values of r_1 and r_2 from a simultaneous fit to the BaBar and CLEO-c branching-fraction measurements. Figure 4 shows the same values. To account for final-state radiation effects in the BaBar measurement, we allow a bias shift between the fit parameters from the BaBar and CLEO-c data. A χ^2 penalty is added for any deviation from the central value for the BaBar corrections, according to their systematic uncertainties on the corrections. The CLEO measurements unfold the reconstructed q^2 distributions back to the pre-FSR distributions, so the corresponding correction is not necessary.

The D^0 and D^+ parameters are in good agreement.

Figure 4: The 68% and 96% probability contours for the BaBar and CLEO-c r_1 and r_2 measurements. The contours from the simultaneous fit to the BaBar and CLEO-c data are also shown.

III. Semileptonic decays to vector mesons

Eq. (7) and Eq. (8) described $D \to V\ell\nu$ decay rates in terms of the form factors $H_\pm(q^2)$ and $H_0(q^2)$ for the three helicity states of the W boson. In terms of angles defined in Fig. 1, where the vector meson decays to two pseudoscalars, we have

$$\frac{d\Gamma(P \to V l\nu, V \to P_1 P_2)}{dq^2 d\cos\theta_V d\cos\theta_l d\chi} = \frac{3G_F^2}{2048\pi^4}|V_{cq}|^2 \frac{p^*(q^2)q^2}{M_D^2}\mathcal{B}(V \to P_1P_2)$$
$$\Big\{ (1+\cos\theta_l)^2 \sin^2\theta_V |H_+(q^2)|^2$$
$$+ (1-\cos\theta_l)^2 \sin^2\theta_V |H_-(q^2)|^2 + 4\sin^2\theta_l \cos^2\theta_V |H_0(q^2)|^2$$
$$+ 4\sin\theta_l(1+\cos\theta_l)\sin\theta_V\cos\theta_V\cos\chi H_+(q^2)H_0(q^2)$$
$$- 4\sin\theta_l(1-\cos\theta_l)\sin\theta_V\cos\theta_V\cos\chi H_-(q^2)H_0(q^2)$$
$$- 2\sin^2\theta_l\sin^2\theta_V\cos 2\chi H_+(q^2)H_-(q^2)\Big\}. \tag{15}$$

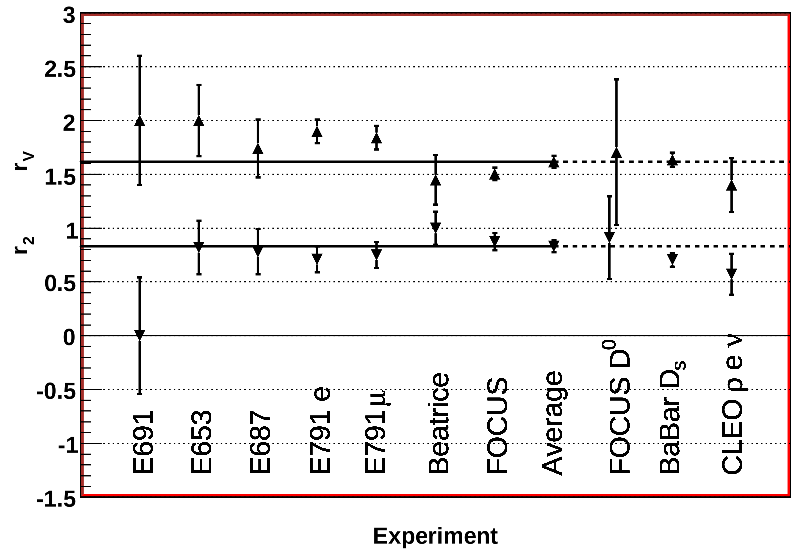

Figure 5: A comparison of r_V and r_2 values. The first set of measurements are for $D^+ \to K^-\pi^+l^+\nu_l$ decays. Plotted next is the average of these measurements, followed by measurements in D^0 decays, D_s^+ decays and Cabibbo-suppressed D^+ decays.

Assuming that the simple-pole form of Eq. (10) describes the q^2-dependence of the form factors $V(q^2)$, $A_1(q^2)$, and $A_2(q^2)$, the 4-dimensional distribution given by Eq. (7) depends only on the ratios

$$r_V \equiv V(0)/A_1(0), \qquad r_2 \equiv A_2(0)/A_1(0), \tag{16}$$

which are the most frequently reported decay parameters.

Figure 5 and Table 3 give measurements of r_V and r_2 for $D \to V\ell\nu$ decays (mostly $D^+ \to \overline{K}^{*0}\ell^+\nu$ decays). The measurements are in good agreement; even the Cabibbo-suppressed modes and the D^0 and D_s^+ decays agree with the average of the D^+ decay results. But is the quality of the fits good? The BaBar D_s^+ results and the FOCUS results have the highest statistics. The BaBar pre-publication [26] does not quote a goodness-of-fit, but the fit projections show that the fit is

Table 3: Results for r_V and r_2.

$D^+ \to \overline{K}^{*0}\ell^+\nu$ Expt.	Ref.	r_V	r_2
E691	[18]	$2.0 \pm 0.6 \pm 0.3$	$0.0 \pm 0.5 \pm 0.2$
E653	[19]	$2.00 \pm 0.33 \pm 0.16$	$0.82 \pm 0.22 \pm 0.11$
E687	[20]	$1.74 \pm 0.27 \pm 0.28$	$0.71 \pm 0.08 \pm 0.06$
E791 (e)	[21]	$1.90 \pm 0.11 \pm 0.09$	$0.71 \pm 0.08 \pm 0.09$
E791 (μ)	[22]	$1.84 \pm 0.11 \pm 0.09$	$0.75 \pm 0.08 \pm 0.09$
Beatrice	[23]	$1.45 \pm 0.23 \pm 0.07$	$1.00 \pm 0.15 \pm 0.03$
FOCUS	[24]	$1.504 \pm 0.057 \pm 0.039$	$0.875 \pm 0.049 \pm 0.064$
Average		1.62 ± 0.055	0.83 ± 0.054
FOCUS $D^0 \to \overline{K}^0\pi^-\mu^+\nu$	[25]	$1.706 \pm 0.677 \pm 0.342$	$0.912 \pm 0.370 \pm 0.104$
BaBar $D_s^+ \to \phi e^+\nu$	[26]	$1.636 \pm 0.067 \pm 0.038$	$0.705 \pm 0.056 \pm 0.029$
CLEO $D^0, D^+ \to \rho e\nu$	[27]	$1.40 \pm 0.25 \pm 0.03$	$0.57 \pm 0.18 \pm 0.06$

acceptable. And FOCUS obtains an acceptable χ^2-based probability of 5.2% when a $\overline{K}\pi$ S-wave is included.

Evidence for an S-wave component in vector decays

The evidence from FOCUS for an S-wave component is an asymmetry in the decay amplitude in the cos θ_V distribution [28]. Including a constant S-wave amplitude of the form $Ae^{i\delta}$ in Eq. (15) leads to an interference term proportional to $|AH_0 \sin\theta_l \cos\theta_V|$, which can be seen as an asymmetry in the roughly $\cos^2\theta_V$ form of the differential distribution caused by the dominance of H_0 compared to $H_\pm$.

With the S-wave amplitude included, FOCUS finds that the fit improves markedly; the S-wave amplitude and phase are $A = 0.330 \pm 0.022 \pm 0.015$ GeV^{-1} and $\delta = 0.68 \pm 0.07 \pm 0.05$ [24].

Model-independent form factor measurements

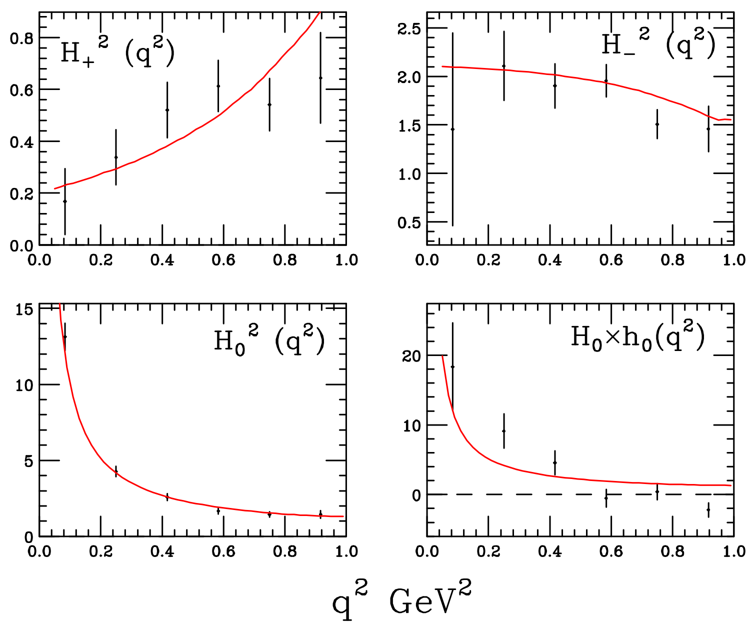

Figure 6: Model-independent form factors from CLEO-c.

CLEO-c has extracted model-independent form factors [29] in $D^+ \to K^-\pi^+e^+\nu_e$ decays, shown in Fig. 6: $H_0(q^2)$ clearly dominates, especially at low q^2. Even though the $K\pi$ mass distribution appears to be completely dominated by the $K^*(892)$, a fairly good determination, via the interference term, of the S-wave form factor $h_0(q^2)$ is also obtained. At the moment, the D-wave and S-wave components appear to be smaller than the S-wave. Higher statistics data from BaBar and Belle may reveal deficiencies in the pole model.

***z* expansions for vector decay**

CLEO-c has also made the "Hill transformation" from q^2 to the z variable. In the narrow allowed range of z, the transformed H_0 data are consistent with being constant, indicating that the transformation works well as a way of describing vector form-factors.

References

1. T. Becher and R.J. Hill, Phys. Lett. **B633**, 61 (2006).

2. M. Kobayashi and T. Maskawa, Prog. Theor. Phys., **49**, 652, (1973).
3. F.J. Gilman and R.L. Singleton, Phys. Rev. **D41**, 142 (1990).
4. C.G. Boyd, B. Grinstein, and R.F. Lebed, Phys. Rev. Lett. **74**, 4603 (1995).
5. R.J. Hill, `hep-ph/0606023` (2006).
6. D. Becirevic and A.B. Kaidalov, Phys. Lett. **B478**, 417 (2000).
7. C.G. Boyd and M.J. Savage, Phys. Rev. **D56**, 303 (1997).
8. M.C. Arnesen *et al.*, Phys. Rev. Lett. **95**, 071802 (2005).
9. C. Bourrely, B. Machet, and E. de Rafael, Nucl. Phys. **B189**, 157 (1981).
10. J.M. Link *et al.*, Phys. Lett. **B607**, 233 (2005).
11. G.S. Huang *et al.*, Phys. Rev. Lett. **94**, 011802 (2005).
12. L. Widhalm *et al.*, Phys. Rev. Lett. **97**, 061804 (2006).
13. B. Aubert *et al.*, Phys. Rev. **D76**, 052005 (2007).
14. Y. Gao, Talk presented at the *XXXIII International Conference on High Energy Physics (ICHEP'06)*, Moscow, the Russian Federation, August 2006.
15. D. Cronin-Hennessy *et al.*, `arXiv:0712.0998 [hep-ex]` (2007).
16. S. Dobbs *et al.*, `arXiv:0712.1020 [hep-ex]` (2007).
17. C. Aubin *et al.*, Phys. Rev. Lett. **94**, 011601 (2005).
18. J.C. Anjos *et al.*, Phys. Rev. Lett. **65**, 2630 (1990).
19. K. Kodama *et al.*, Phys. Lett. **B274**, 246 (1992).
20. P.L. Frabetti *et al.*, Phys. Lett. **B307**, 262 (1993).
21. E.M. Aitala *et al.*, Phys. Rev. Lett. **80**, 1393 (1998).
22. E.M. Aitala *et al.*, Phys. Lett. **B440**, 435 (1998).
23. M. Adamovich *et al.*, Eur. Phys. J. **C6**, 35 (1999).
24. J.M. Link *et al.*, Phys. Lett. **B544**, 89 (2002).
25. J.M. Link *et al.*, Phys. Lett. **B607**, 67 (2005).
26. B. Aubert *et al.*, `hep-ex/0607085` (2006).
27. H. Mahlke, `hep-ex/0702014`, (2007).
28. J.M. Link *et al.*, Phys. Lett. **B535**, 43 (2002).
29. M.R. Shepherd *et al.*, Phys. Rev. **D74**, 052001 (2006).